Nonlinear emission from a ferrite in ferromagnetic resonance

G. A. Melkov and A. Yu. Taranenko

T. G. Shevchenko Kiev State University

(Submitted 18 February 1986)
Zh. Eksp. Teor. Fiz. **91**, 1007–1015 (September 1986)

Electromagnetic emission has been detected from a ferrite in ferromagnetic resonance at the frequency of a pump in the 3-cm range. The test samples were single-crystal spheres of yttrium iron garnet. The emission was noisy, with frequencies concentrated in two spectral regions below the pump frequency. The reason for this emission may be a kinetic instability of spin waves.

INTRODUCTION

The processes which occur in magnetically ordered crystals pumped by a microwave power P above the threshold P_{thr} for the parametric excitation of spin waves are now understood quite well. The theory which has been derived, and which incorporates three- and four-wave interactions of parametrically excited spin waves (PESW) with each other and with the pump field, gives a completely satisfactory description of the behavior of ferrites and antiferromagnets at values of the power scaled by the threshold value up to $\zeta = P/P_{\text{thr}} \sim 10$ dB (Refs. 1–3). Research on ferrites at higher values of the scaled pump power ($\zeta \sim 15$ dB) during the parametric excitation of spin waves at a frequency ω_k equal to half the pump frequency ω_p (the first-order parametric process) resulted in the observation of a new kinetic instability of spin waves, in which the primary spin waves parametically excited by the pump themselves serve as pumps which generate secondary spin waves.[4,5] In the present paper we report a study of the behavior of ferrites at high pump power levels under different conditions—in the absence of parametric excitation of spin waves at the frequency $\omega_k = \omega_p/2$, which is forbidden by energy conservation, but in the presence of second-order parametric processes, which give rise to the excitation of spin waves with a frequency equal to the pump frequency, $\omega_k = \omega_p$. In order to identify these conditions, the ferrite must be in a static magnetic field H close to the ferromagnetic-resonance (FMR) field H_0 at the pump frequency ω_p. Furthermore, the frequency $\omega_p/2$ should lie below the lower boundary of the spin-wave spectrum in order to prevent the possible occurrence of second-order processes. For spherical samples of yttrium iron garnet (YIG) at room temperature, the pump frequency would accordingly have to satisfy the condition $(\omega_p/2\pi) > 3.3$ GHz (§8 in Ref. 6). This is the most interesting case in practice. For example, ferrite filters are always operated under ferromagnetic resonance conditions, $H \approx H_0$, at signal frequencies which rule out a first-order parametric process in order to improve the efficiency and to increase the maximum working power.[7]

Experiments carried with spherical YIG samples with a pump in the 3-cm wavelength range have revealed electromagnetic emission from the ferrite at frequencies below the pump frequency. The emission appears once a threshold has been reached in the pump power: $\zeta = \zeta_0 > 6$ dB.

EXPERIMENTAL PROCEDURE

1. Figure 1 is a block diagram of the experimental apparatus. The pump power of frequency ω_p, from the 3-cm-range magnetron source M, passes through an isolator, a precision attenuator PA_1, and a bidirectional coupler BC to the measurement section MS, which is immersed in a static magnetic field. The measurement section is a short-circuited length of a standard rectangular 3-cm-range waveguide, in which the spherical YIG single-crystal test sample is placed at an antinode of the alternating magnetic field **h**. The static magnetic field **H** is directed perpendicular to the wide wall of the waveguide and to the vector **h** at the position of the ferrite. For a study of the signal radiated by the ferrite, the ferrite is surrounded by a wire loop, connected to coaxial cable. The plane of the loop is parallel to **h**, so that the effect on the pump field is eliminated. The bidirectional coupler, along with the waveguide switch Sw, the precision attenuator PA_2, and the oscilloscope O_1, is used to measure the susceptibility of the ferrite and the power absorbed in it. It is also used to tune the magnetic field to resonance with the pump frequency. The precision attenuator PA_1 is used to establish the necessary level of the pump power P incident on the measurement section. The threshold power for the excitation of spin waves, P_{thr}, required for determining the reduced pump power $\zeta = P/P_{\text{thr}}$, is determined by the method of Green and Schloemann (§20 in Ref. 6), from the experimental dependence of the imaginary part of the resonant susceptibility of the ferrite, $\chi''(H_0) = \chi''_{\text{res}}$, on the pump power.

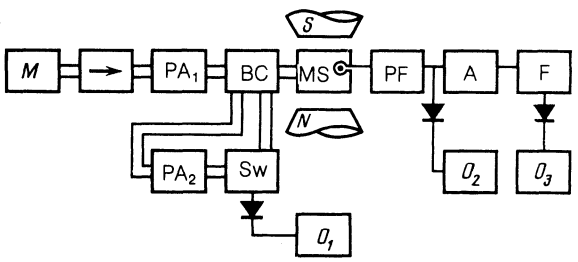

FIG. 1. Block diagram of the experimental apparatus. M—Magnetron source; PA—precision attenuator; BC—bidirectional coupler; Sw—waveguide switch; MS—measurement section with the ferrite; PF—pump filter; O—oscilloscope; A—microwave amplifier; F—frequency meter.

 0038-5646/86/090592-06$04.00

The second-order parametric instability gives rise to spin waves with a frequency equal to the pump frequency. These waves propagate along the static magnetic field; i.e., they have polar angles $\theta_k = 0$ and π (Ref. 8). The wave vector of the parametrically excited spin waves does not depend on the pump frequency.[8] For the YIG ferrite sphere at room temperature we have $k = 3.5 \cdot 10^5$ cm^{-1}.

The microwave signal emitted by the ferrite is sent by the wire loop and coaxial cable through a coaxial pump filter (PF) to the measurement circuit, where its magnitude and the pulse shape are measured, and its spectral composition is studied. The first two parameters of the signal are measured with oscilloscope O_2. Its spectrum is determined by means of a feed-through resonant frequency meter F with a bandpass of 10 MHz and oscilloscope O_3. To study the spectral composition of the signal, we also use an S4-27 spectrum analyzer, but because of the pulsed nature of the signal and the low pulse repetition frequency the use of this analyzer increases the measurement time. Ultimately, this increase in time degrades the accuracy of the measurements because of the fluctuations of the field of the electromagnet and of the magnetron power. Interchangeable units make it possible to achieve a sensitivity $\sim 10^{-10}$ W for the measurement circuit over the frequency range 1.9–12 GHz. The pump filter is used to prevent the intense pump pulse from affecting the measurement circuit. This filter consists of a band-rejection filter with a 50-MHz rejection band and with an attenuation at the pump frequency ω_p of at least 60 dB.

Most of the measurements were carried out with a 9370-MHz magnetron source with a maximum power $P_M \sim 1$ kW, a pulse length $\tau = 2$ μs, and a pulse repetition frequency $F = 10G$ Hz. To study the susceptibility of the ferrite, the shape of the pulses, and the shape of the absorption lines, we use a low-power magnetron at the frequency 9430 MHz with $\tau = 104$ μs, $P_M \sim 15$ W, and $F = 10$ Hz. The diameter of the test spheres is in the range 1.5–2.89 mm. The natural width of the FMR lines, ΔH_0, is ~ 0.5 Oe for all of these spheres. The coupling loop and the waveguide of the measurement section make the total width ΔH of the FMR line several times larger. For the largest sphere, 2.89 mm in diameter, this width is $\Delta H \sim 4$ Oe. The results found for all of the samples differ only in the magnitude of the effect. For example, the radiated power is approximately proportional to the square of the volume of the sample. These spheres are oriented with their [111] easy axis along the direction of the static magnetic field.

2. The search for nonlinear emission from the ferrite was carried out over the entire pump power range 0–1 kW and over the entire frequency range of the measurement circuit, 1.9–12 GHz. Emission of this type was detected for all of the single-crystal YIG spheres studied. The emission arises when a threshold is reached in the reduced pump power, $\zeta < \zeta_0$, and is of a noisy nature. The value of ζ_0 varies over the range 6–8 dB for the various samples. The emitted power depends in a resonant fashion on the static magnetic field; the maximum of the emission is usually shifted a few oersteds above the FMR field H_0. Figure 2 shows the maximum radiated power P_r as a function of the reduced pump power

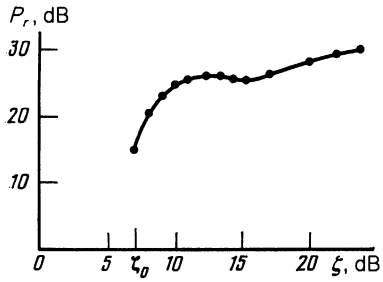

FIG. 2. Maximum power of the nonlinear emission, P_r, versus the reduced pump power ζ at $H = H_0$. The origin for the decibel scale on the ordinate axis corresponds to $(1.1 \pm 0.5) \cdot 10^{-6}$ W. The sample is a single-crystal sphere of yttrium iron garnet, 2.89 mm in diameter. The pump frequency is 9370 MHz.

for one of the samples. Immediately after the emission threshold ζ_0 is exceeded, the power P_r reaches values of a few tens of microwatts and is easily seen on the screen of oscilloscope O_2 (Fig. 1), even without additional amplifiers. As the pump power is raised further, the power of this emission increases on the average, although for some samples there is a slight minimum at $\zeta \sim 15$ dB on the $P_r = f(\zeta)$ curve (Fig. 2). The maximum power of the emission at a pump power $P \sim 10^3$ W and for the largest sphere, 2.89 mm in diameter, is on the order of 1 mW. For the other spheres, this power decreases roughly in proportion to the square of their volume.

3. Figure 3 shows the spectrum of the emission of the ferrite. It is seen to consist of two components, with frequencies ω_1 and ω_2 satisfying $\omega_1 < \omega_2 < \omega_p$. The width of each component, Δf_1 or Δf_2, is 10–20 MHz when the reduced pump power is just above the threshold. The frequencies ω_1 and ω_2 depend on the diameter of the sphere, the static field H, and the reduced pump power ζ. There is no harmonic relationship of any sort of these frequencies with each other or with the pump frequency. For the case shown in Fig. 3 we have $\omega_1/2\pi \approx 8.8$ GHz, $\omega_2/2\pi \approx 9.22$ GHz, and a pump frequency $\omega_p/2\pi \approx 9.37$ GHz. Figure 4 shows the positions of the emission frequencies with respect to the characteristic frequencies of the ferromagnetic sample. The two spectral components of the emission, at ω_1 and ω_2, appear simultaneously in the case $\zeta \geqslant \zeta_0$, but when the pump power is just

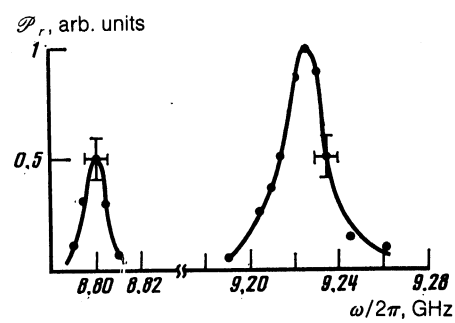

FIG. 3. The spectral density ($\mathscr{P}_r$) of the nonlinear emission versus the frequency for a single-crystal sphere of yttrium iron garnet 2.89 mm in diameter ($H_0 = 3380$ Oe, $H = 3383$ Oe, $\zeta = 12$ dB).

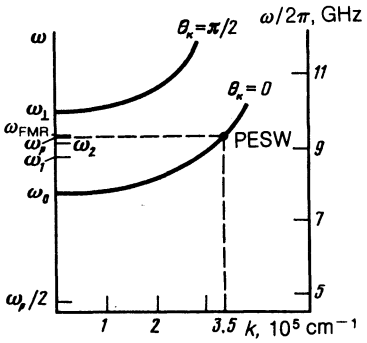

FIG. 4. Positions of the emission frequencies ω_1 and ω_2 in the spectrum of spin-wave oscillations of the ferrite for the conditions of the experiments whose results are shown in Fig. 3. ω_1—upper boundary of the spin-wave spectrum in the limit $k \to 0$; ω_p—frequency of the pump and of the (PESW) parametrically excited spin waves; ω_{FMR}—FMR frequency; ω_0—minimum frequency of the spin-wave spectrum.

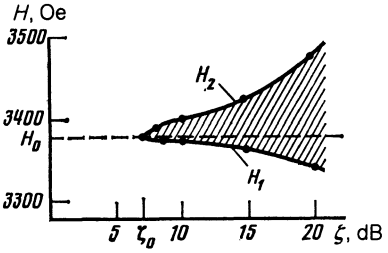

FIG. 5. The hatching shows the region in which the nonlinear emission from the ferrite occurs. The sample is a single-crystal sphere of yttrium iron garnet 2.89 mm in diameter. $H_0 = 3380$ Oe; H_1 and H_2 are the boundaries of the region in which the image now occurs.

above the threshold the spectral density of the low-frequency component (ω_1) is significantly lower than that of the high-frequency component. With a further increase in the pump power, however, the two spectral densities become equal. According to Fig. 3, for example, the ratio of the maxima of the spectral densities of the two components at $\zeta = 12$ dB is ~ 2, but at $\zeta = 16$ dB it is less than 1.5.

Both spectral components are detected from all of the samples, except the smallest sphere, 1.5 mm in diameter. In that case we detect only the high-frequency component, and even that component is at the sensitivity limit of the apparatus because of the small volume of the sphere.

The width of the high-frequency emission peak, Δf_2 is greater than Δf_1 in all cases. At the highest values of the reduced pump power, the width Δf_2 reaches 100 MHz, while Δf_1 is less than 30 MHz.

4. Nonlinear emission from the ferrite occurs near the FMR field H_0 in a limited interval of the static magnetic field H. The width δH of this interval depends on the reduced pump power. As H increases, the emission appears abruptly at the field H_1 and then disappears abruptly at $H_2 = H_1 + \delta H$. At $\zeta = \zeta_0$, we find $H_1 \approx H_2 \approx H_0 + \Delta H_0$ in the limit $\delta H \to 0$; i.e., when the pump power is just above the threshold, the emission arises on the right-hand slope of the resonance curve ($H > H_0$). With increasing reduced pump power, the interval in which the emission occurs initially spans the entire resonance curve; later on (at $\zeta \gtrsim 25$ dB), the width δH of this interval reaches values of a few hundred oersteds. Figure 5 shows an example of how the region in which the nonlinear emission from the ferrite occurs depends on the reduced pump power for one of the test samples.

Inside the region in which the emission occurs, the spectral density of the high-frequency component of the emission depends only slightly on the strength of the static magnetic field. For the low-frequency component, the spectral density is significant only at $H \lesssim H_1 + 20$ Oe, i.e., near the lower boundary of the region in which the emission occurs. As a result (for example), at the field H_0 it is possible to detect both spectral components of the emission only up to $\zeta \leqslant 17$ dB. At higher values of the reduced pump power, only the high-frequency component of the emission is observed in this field.

5. As the magnetic field is varied over the interval in which the emission occurs, the emission frequencies of both spectral components change. At emission frequencies which are more than ~ 100 MHz below the pump frequency, there is a linear relationship between the radiated power and the field, with a proportionality factor which is approximately equal to the gyromagnetic ratio for the electron spin, γ. This dependence subsequently reaches saturation, and the frequency of the nonlinear emission is below the pump frequency, regardless of the conditions. Figure 6 shows a typical plot of the frequency of the emission in the high-frequency spectral component versus the static magnetic field. It must be kept in mind here that the absence of frequencies $\omega_p/2\pi + 50$ MHz from the emission spectrum may be an instrumental effect, due to the rejection filter at the pump frequency in the measurement circuit.

6. In the final stage of the experiments, we attempted to detect the effect of the processes which lead to the nonlinear emission from a ferrite on the parameters of the ferromagnetic resonance. Because of their major practical importance, the nonlinear properties of ferrites in static magnetic fields close to the FMR field H_0 have been the subject of several

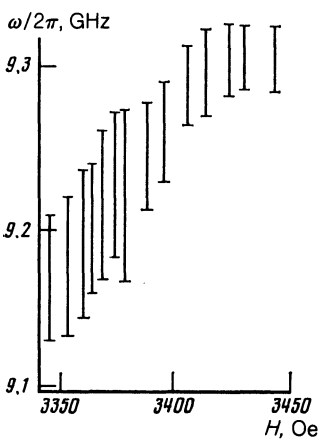

FIG. 6. Frequency of the high-frequency spectral component versus the static magnetic field for an yttrium iron garnet sphere 2.89 mm in diameter. The pump frequency is 9370 MHz; $\zeta = 19$ dB.

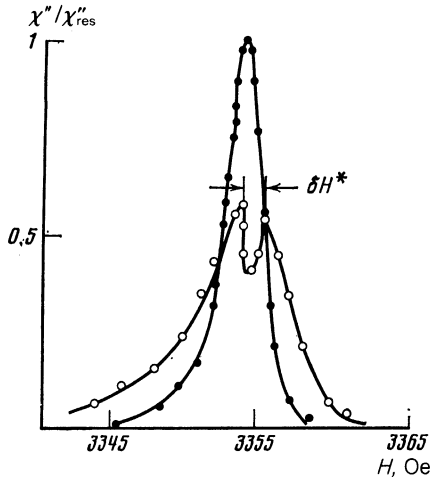

FIG. 7. FMR curve for a single-crystal sphere of yttrium iron garnet 2.26 mm in diameter at various levels of the reduced pump power: ●—$\zeta = -30$ dB; ○—$\zeta = 8$ dB.

studies (§20 in Ref. 6; Ref. 9). A point of particular interest is that these papers have described several experimental results which have yet to be explained. It turns out that the results of the present experiments show that one of these earlier results—the appearance, at a certain reduced pump power $\zeta = \zeta^*$, of a dip on the FMR curve (the plot of the imaginary part of the susceptibility, χ'', of the ferrite versus H; (Ref. 10)—is directly related to the nonlinear emission from the ferrite observed in the present experiments.

Figure 7 shows two experimental curves of $\chi''(H)$, measured for one of the YIG spheres studied in the present experiments, for various pump power levels P. The first of these curves corresponds to the case of a low reduced pump power, $\zeta \ll 1$ ($P \ll P_{\text{thr}}$), at which essentially none of the nonlinear processes are operating in the spin-wave interactions. As the reduced pump power increases, so does the efficiency of these interactions, and at $\zeta \sim 1$ ($P \sim P_{\text{thr}}$) there is a significant broadening of the resonance curve due to the parametric excitation of spin waves with the frequency $\omega_k = \omega_p$. In other words, the FMR reaches saturation. Finally, at reduced pump power levels $\zeta \geqslant \zeta^*$, in the range 6–8 dB for the different samples, the FMR curve becomes a double-humped curve, with a dip at the center of the line. This case corresponds to the second curve in Fig. 7. With a further increase in the reduced pump power, this curve becomes even broader, and the distance δH^* between the humps increase (Fig. 7).

Simultaneous observations of the dip on the FMR curve and of the nonlinear emission from the ferrite revealed that these phenomena always accompany each other. The reduced pump power levels at which they appear and the regions in which they exist are also precisely the same ($\zeta^* = \zeta_0$; $\delta H + \delta H^*$). The apparent meaning is that these two effects are different manifestations of the same nonlinear process.

7. In real crystals, spin waves can effectively interact with an electromagnetic field through magnetostatic magnetization-precession modes.[11] Accordingly, an experimental study was carried of the absorption spectrum of the ferrite near the frequencies ω_1 and ω_2. For this purpose, an R2-601 panoramic meter, capable of measuring the standing-wave ratio over the frequency range 8.15–12.05 GHz, was connected to the waveguide input of the measurement section MS in place of the bidirectional coupler BC (Fig. 1). The strength of the static magnetic field corresponded to the resonant value at the pump frequency ω_p. For samples 2.26 and 2.89 mm in diameter, three resonant absorption peaks were observed below the pump frequency. The frequencies of two of these peaks agreed to within 10 MHz with the frequencies ω_1 and ω_2. The (210) and (300) magnetostatic precession modes correspond to these resonances.[12] The third resonance corresponds to the (310) magnetostatic mode and lies ~ 800 MHz below ω_p. Several resonant absorption peaks were observed at frequencies above the pump frequency—some 50–400 MHz above it. We did not carry out any special studies to detect nonlinear emission at frequencies above the pump frequencies or at the frequency corresponding to the (310) magnetostatic procession mode.

8. All of the experiments described above correspond to the case in which the magnetization of the single-crystal YIG spheres was along the [111] easy axis. When the orientation of the magnetization with respect to the crystallographic axes is changed, the nonlinear emission from the ferrite retains all of its basic characteristics, although certain features change significantly. For example, in the case $\mathbf{H} \| [100]$ the integral emission power remains about an order of magnitude lower than that at the corresponding value of the reduced pump power in Fig. 2, up to $\zeta = 15$ dB. For $\zeta > 15$ dB, however, the emission power increases rapidly, reaching the same values as at $\mathbf{H} \| [111]$.

DISCUSSION OF RESULTS

1. Most of the experimental behavior described above can be explained under the assumption that at pump power levels $\zeta \geqslant \zeta_0$ secondary spin waves arise in the ferrite and are distributed over a broad frequency interval below the pump frequency. The width of this interval is ~ 600 MHz. The excitation of the secondary spin waves leads to a decrease in the susceptibility of the ferrite and therefore the appearance of dips on the resonant curve. As a result of two-magnon processes, the secondary spin waves work through the magnetostatic magnetization-precession modes which are degenerate with them to excite electromagnetic wave with frequencies corresponding to the eigenfrequencies of these precessions, ω_ν. If the distribution of the phases of the secondary spin waves is random, the electromagnetic waves are of a noisy nature. The width of the emission spectrum from a sample should be determined by the width of the line of the magnetostatic modes. The behavior of the emission frequency as a function of the magnetic field H is determined by the H dependence of the frequencies of the magnetostatic precession modes, ω_ν, through which the emission occurs. At $H \gtrsim 4\pi M_0$, where M_0 is the saturation magnetization of the sample, we have $\omega_\nu \sim \gamma$. As the pump power ζ is increased, and as ω_ν and ω_p move close together, the resonance lines of the precession modes broaden; at the same

time, the spectrum of the nonlinear emission from the ferrite broadens.

2. What are the reasons for the appearance of the secondary spin waves? The directs process—the decay of a parametrically excited spin wave (PESW) into two spin waves—was eliminated under the experimental conditions (see the Introduction). The decay of a parametrically excited spin wave into a spin wave and an elastic wave is allowed by energy and momentum conservation, but because of the weak magnetoelastic interaction in YIG this decay has a significant probability at room temperature only at $\zeta > 80$ dB (Ref. 13)—well above the values reached experimentally. The most plausible explanation of the appearance of the secondary spin waves is the kinetic instability of spin waves which is discovered in Ref. 4 in the case of a parallel pumping of a spin-wave instability. As a result of this instability, two primary, parametrically excited spin waves with wave vectors $\mathbf{k}_1$ and $\mathbf{k}_2$ merge, forming two secondary waves with wave vectors $\mathbf{k}'$ and $\mathbf{k}''$. Here we of course have the relations $\mathbf{k}_1 + \mathbf{k}_2 = \mathbf{k}' + \mathbf{k}''$ and $\omega_{k_1} + \omega_{k_2} = \omega_{k'} + \omega_{k''}$. For the case described in Ref. 4 the relations $k_1 \approx k_2$, $k' \gg k'' \approx 0$, $\omega_{k'} \gg \omega_{k''} = \omega_0$ hold, where ω_0 is the lowest-lying frequency in the spin-wave spectrum. As a result of the kinetic instability, the amplitude of the long secondary spin waves increases exponentially at the bottom of the spin-wave spectrum, $\omega_k'' = \omega_0$, which experience the waste damping. Under the conditions of the present experiments, however, processes of this sort with corresponding relations between k_1, k_2 and k', k'' were forbidden by energy and momentum conservation. In view of the distribution of spinwaves which appear as a result of the second-order parametric process in momentum space (the polar angle of the parametrically excited spinwaves is $\theta_k = 0, \pi$; Ref. 8), we can show that the only allowed process which is capable of driving a kinetic instability of spin waves in the present experimental situation is a process in which we have

$$k_1 = -k_2, \quad k' \approx k'' \approx 0, \quad \omega_{k'} + \omega_{k''} = 2\omega_p. \tag{1}$$

For energy conservation, the frequencies $\omega_{k'}$, $\omega_{k''}$ ($\omega_{k'} > \omega_{k''}$) must lie within the spin-wave spectrum in the limit $k \to 0$:

$$\omega_{k'} \leqslant \gamma[H_i(H_i + 4\pi M_0)]^{1/2} = \omega_\perp, \quad \omega_{k''} \geqslant \omega_0, \quad \omega_{k'} + \omega_{k''} = 2\omega_p, \tag{2}$$

where H_i is the static internal magnetic field; for a sphere, it would be $H_i = H - (4/3)\pi M_0$.

In our experiments, the frequency $\omega_\perp$ was ~ 670 MHz above the frequency of the FMR, $\gamma H_0 \propto \omega_{\text{FMR}}$. Consequently, the frequencies of the secondary spinwaves, $\omega_{k''}$, cannot be more than 670 MHz below the pump frequency ω_p, according to (2). This conclusion agrees well with the experimental results: there is a nonlinear emission from the ferrite through magnetostatic precession modes whose eigenfrequencies lie 150 and 570 MHz below the pump frequency, but this emission does not occur for precession at the frequency $\omega_\nu = \omega_p - 800$ MHz.

The presence of the wide spectrum of secondary spin waves, with a width an order of magnitude greater than in the case of parallel pumping, may be a consequence of the fact that the secondary spin waves include no waves with a clearly defined minimum of the damping, such as secondary spin waves which lie at the bottom of the spin-wave spectrum. In this case the instability threshold will of course be reached simultaneously for a set of secondary spin waves which is larger than in the case of parallel pumping.

Another point which is not clear is the absence, within 10^{-10} W, of nonlinear emission from the ferrite at frequencies above the pump frequency. This result seems to mean that the amplitudes of the secondary spin waves at frequencies $\omega_{k'} > \omega_p$ are significantly lower than the amplitudes of the secondary spin waves at frequencies $\omega_{k''}$ below the pump frequency. This would represent a substantial contrast with the case of the kinetic instability of spin waves during parallel pumping,[4] where the differences among the amplitudes of the secondary spin waves are insignificant, on the order of the ratio of their damping levels. A difference of this sort may be due to a difference in the processes which drive the kinetic instabilities of the spin waves in these two cases. According to (1), both the parametrically excited spinwaves and the pump itself directly affect the excitation of secondary spinwaves at an FMR. The pump wave factor approximately vanishes, so that there can be processes involving a splitting of the pump oscillations into spin waves which satisfy conditions (1). In the case of parallel pumping, only the parametrically excited spin waves have a direct effect on the excitation of secondary spin waves: The pump in this case cannot interact directly with the secondary spin waves, because such an interaction is forbidden by energy and momentum conservation. Accordingly, the case of the kinetic instability of spin waves at an FMR is closer to the case of the kinetic instability of spin waves under the influence of two pumps.[14] The same circumstance can explain why the kinetic instability during the FMR set in at a reduced pump level, 8–10 dB lower than in the case of parallel pumping. It is thus clear that a more detailed explanation of the experimental results must await the development of a theory for the kinetic excitation of spinwaves at FMR.

CONCLUSION

The nonlinear phenomena which occur in single-crystal ferromagnetic spheres of yttrium iron garnet in ferromagnetic resonance at the pump frequency have been studied experimentally. Under conditions such that there is no first-order parametric process, electromagnetic emission has been observed from the ferrite at discrete frequencies below the pump frequency. This emission arises after a threshold is reached, when the pump power is raised to a value 6–8 dB above the threshold for the excitation of spin waves with a frequency equal to the pump frequency. This emission is of a noisy nature. Its spectral characteristics depend on the strength of the static magnetic field, the diameter of the sample, and the pump power. The emission is accompanied by the appearance of a dip on the ferromagnetic-resonance curve.

It has been suggested that the reason for these phenomena is a kinetic instability of secondary spin waves which is

driven by the primary, parametrically excited waves with oppositely directed wave vectors. The secondary spin waves exist over a broad frequency range below the pump frequency. The width of this range is determined by energy and momentum conservation for the interacting waves. The electromagnetic emission from the ferrite occurs as a result of the excitation of magnetostatic precession modes of the sample by the secondary spin waves through two-magnon scattering processes.

We wish to thank V. S. L'vov and V. B. Cherepanov for a useful discussion.

[1]V. E. Zakharov, V. S. L'vov, and S. S. Starobinets, Zh. Eksp. Teor. Fiz. **114**, 609 (1974) [Sov. Phys. JETP **17**, 896 (1975)].
[2]L. A. Prozorova and A. N. Smirnov, Zh. Eksp. Teor. Fiz. **67**, 1952 (1974) [Sov. Phys. JETP **40**, 970 (1975)].
[3]G. A. Melkov and I. V. Krutsenko, Zh. Eksp. Teor. Fiz. **72**, 564 (1977) [Sov. Phys. JETP **45**, 295 (1977)].
[4]A. V. Lavrinenko, V. S. L'vov, G. A. Melkov, and V. B. Cherepanov, Yad. Fiz. **81**, 1022 (1982) [Sov. J. Nucl. Phys. **54**, 542 (1981)].
[5]A. V. Lavrinenko, G. A. Melkov, and A. Yu. Taranenko, Fiz. Tverd. Tela (Leningrad) **26**, 1499 (1984) [Sov. Phys. Solid State **26**, 910 (1984)].
[6]Ya. A. Monosov, Nelineĭnyĭ ferromagnitnyĭ rezonans (Nonlinear Ferromagnetic Resonants), Nauka, Moscow, 1971.
[7]M. E. Il'tsenko, G. A. Melkkov, and G. A. Mirskikh, Tverdotel'nye SVCh fil'try (Solid-State Microwave Filters), Tekhnika, Kiev, 1977.
[8]H. Suhl, Phys. Chem. Sol. **1**, 209 (1957).
[9]A. G. Gurevich, Ferrity na sverkhvysokikh chastotakh (Ferrites at Microwave Frequencies), Fizmatgiz, Moscow, 1960.
[10]S. S. Starobinets and A. G. Gurevich, J. Appl. Phys. **39**, 1075 (1968).
[11]I. V. Krutsenko, V. S. L'vov and G. A. Melkov, Zh. Eksp. Teor. Fiz. **75**, 114 (1978) [Sov. Phys. JETP **48**, 56 (1978)].
[12]P. C. Fletcher and R. O. Bell, Appl. Phys. **30**, 687 (1959).
[13]G. E. Fal'kovich, Preprint No. 172, Institute of Automation and Electrometry, Siberian Branch, Academy of Sciences of the USSR, Novosibirsk, 1983.
[14]A. V. Lavrinenko, G. A. Melkov, and G. E. Fal'kovich, Zh. Eksp. Teor. Fiz. **87**, 205 (1984) [Sov. Phys. JETP **60**, 118 (1984)].

Translated by Dave Parsons